A PROPOSED HANGUP FREE AND SELF-NOISE REDUCTION METHOD FOR DIGITAL SYMBOL SYNCHRONISER IN MFSK SYSTEMS

C.D. LEE and M. DARNELL
Institute of Integrated Information Systems
School of Electronic and Electrical Engineering,
The University of Leeds, LS2 9JT, UK.

Abstract-The contribution of this paper is concerns digital symbol synchronisers for MFSK systems. Methods are proposed to achieve hangup free operation and to reduce self-noise. Symbol synchronisation hangup can be detected and acquisition time can be reduced if all the samples per symbol from the matched filter output are used. A phase-modulated-M-ary-frequency-shift-keying (PM-MFSK) scheme is introduced to reduce self-noise due to random data. In the analysis, the timing error variances of the symbol synchronisers developed are derived. The synchronisers are evaluated via acquisition time required and timing error variance under additive white Gaussian noise (AWGN) channel conditions.

I. INTRODUCTION

Most symbol synchronisers have been analysed for M-ary phase-shift-keying (MPSK) or quadrature amplitude modulation (QAM) [1]-[4]. The implementation of a symbol synchroniser for MFSK is slightly different from MPSK because the former has M basis functions, which means each signaling tone is a basis function. Hence, we need to implement M matched filters in parallel so that each can be matched to a particular signaling tone. Coherent detection is used here and perfect carrier synchronisation is assumed. Symbol synchronisation hangup and self-noise are the common problems faced by symbol synchronisers. Synchronisation hangup is a phenomenon that occurs when normalised timing error is close to 0.5 (i.e. the unstable equilibrium point); it will tend to move to a stable point but, in doing so, its evolution will be governed by noise since the steering force S-curve is small. As a result, the occurrence of a hangup gives rise to a long acquisition time. Both thermal noise and self-noise contribute to timing error variance. The former dominates at small SNR and the latter dominates at high SNR. The presence of self-noise is due to the random data. This paper is divided into sections as follows: section II describes the operation of the digital symbol synchroniser; section III shows how synchronisation hangup can be detected and corrected; section IV illustrates how self-noise can be reduced; the performance of the proposed synchroniser is analysed in section V and evaluated in section VI; finally, in section VII, we conclude the paper.

II. DIGITAL SYMBOL SYNCHRONISER

After the symbol synchroniser has obtained the initial estimate from a known sequence, the detection process can be started. Consequently, the estimated sequence $\hat{\boldsymbol{c}}$ can be used to remove data dependency. This method is called decision-directed (DD) synchronisation algorithm and is given by

$$\hat{\tau} = \arg \max_{\tilde{\tau}} p(r \mid \tilde{\mathbf{c}} = \hat{\mathbf{c}}, \tilde{\tau}) \qquad (1)$$

The log-likelihood function is given by [2]

$$L(r \mid \tilde{\tau}, \tilde{\mathbf{c}}) = \sum_{m=0}^{(L_0-1)N-1} \mathrm{Re}\left\{r(mT_s)s^*(mT_s, \tilde{\tau})\right\} - \frac{1}{2}\left|s(mT_s, \tilde{\tau})\right|^2 \qquad (2)$$

where L_0 is the observation length in symbols. The $s(mT_s, \tilde{\tau})$ is the trial signal given by

$$s(mT_s, \tilde{\tau}) = \sum_{k=-\infty}^{\infty} \hat{c}_k(mT_s) \cdot g\left(mT_s - kT - \tilde{\tau}\right) \qquad (3)$$

where $\hat{\mathbf{c}}$ represents estimated signaling data sequence, $g(t)$ is a real-valued pulse, and $\tilde{\tau}$ is the generic channel delay. However, the second term is usually dropped because the integral of the term has only a small variation with $\tilde{\tau}$ [2]-[3]. Thus, the approximate log-likelihood function is given by

$$L(r \mid \tilde{\tau}, \tilde{\mathbf{c}}) \approx \sum_{m=0}^{(L_0-1)N-1} \mathrm{Re}\left\{r(mT_s)s^*(mT_s, \tilde{\tau})\right\} \qquad (4)$$

Substituting in (4) from (3), (4) can be written as

$$L(r \mid \tilde{\tau}, \tilde{\mathbf{c}}) \approx \sum_{m=0}^{(L_0-1)N-1} \sum_{k=-\infty}^{\infty} \mathrm{Re}\left\{r(mT_s) \cdot \hat{c}_k^*(mT_s) \right.$$
$$\left. \cdot g\left(mT_s - kT - \tilde{\tau}\right)\right\} \qquad (5)$$

Here we make an approximation that is valid, especially when the observation interval is much longer than the duration of the pulse $g(t)$ [1]. It consists of increasing the summation over m to $\pm \infty$ while restricting the summation over k from 0 to $L_0 - 1$. Hence, (5) can be approximated to

$$\sum_{m=0}^{(L_0-1)N-1} \text{Re}\left\{r(mT_s) \cdot s^*(mT_s, \tilde{\tau})\right\} \approx \sum_{k=0}^{L_0-1} y(kT + \tilde{\tau}, \hat{c}_k)$$

$$(6)$$

where $y(t)$ is the response of $r(t)$ to the matched filter $s(t)$ and is given by

$$y(kT+\tilde{\tau}) = \sum_{m=-\infty}^{\infty} \text{Re}\left\{r_k(mT_s) \cdot \hat{c}_k^*(mT_s) \cdot g(mT_s - kT - \tilde{\tau})\right\}$$

$$(7)$$

Thus,

$$L(r \mid \tilde{\tau}, \tilde{\mathbf{c}}) \approx \sum_{k=0}^{L_0-1} y(kT + \tilde{\tau}, \hat{c}_k) \qquad (8)$$

A DD ML timing parameter estimator is a timing parameter estimator that maximises (8). The log-likelihood function for DD-MDS is defined as

$$\sum_{k=0}^{L_0-1} y(kT + \tilde{\tau}, \hat{c}_k) \approx \sum_{k=0}^{L_0-1} \max_{{}^i\tilde{c}_k}\left(y(kT+\tilde{\tau}, {}^i\tilde{c}_k)\right)$$

$$\text{for } i = 1, ..., M \qquad (9)$$

where ${}^i\tilde{c}_k$ is the ith signaling tone in the alphabet set at k^{th} interval. The DD ML symbol synchroniser here is implemented differently from the one for MPSK [1]-[4] because, in MFSK, the generic data waveform $\tilde{c}$ is not constant within a symbol period. The basic concept of the tracking-loop implementation is to search for the τ that causes the differential of the approximate log-likelihood function to be zero:

$$\frac{\partial \Lambda(\tilde{\tau})}{\partial \tilde{\tau}} = 0 \qquad (10)$$

The structure of the modified tracking-loop MDS (MTMDS) is shown in Figure 1. In tracking-loop MDS (TMDS), the synchronisation epoch is determine by the position of the zero in the differential buffer. Consequently, following from (9) and (10) the ML estimate for the MTMDS with exponential memory is the $\tilde{\tau}$ that satisfies (11)

$$\frac{\partial}{\partial \tilde{\tau}}\left[\frac{1}{L_a}\sum_{k=0}^{\infty}\left(\frac{L_a-1}{L_a}\right)^k \max_{{}^i\tilde{c}_k}\left(y(kT+\tilde{\tau}, {}^i\tilde{c}_k)\right)\right] = 0 \qquad (11)$$

$$\text{for } i = 1, ..., M$$

where L_a is the averaging filter memory. The averaging filter is an infinite impulse response (IIR) filter with feedback gain of $(L_a\text{-}1)/L_a$. The implementation of the averaging filter requires the assumption that the sampling rate is very close to an integer multiple of symbol rate. The interpolator is used for fine timing adjustment. According to (11), the decision-directed unit (DDU) chooses the matched filter output that has the maximum amplitude. By choosing the maximum amplitude, the DDU has indirectly made a symbol decision at every sampling

instant; those symbol decisions are stored in the symbol buffer. The timing error detector is a differential operator. The loop filter updates the timing estimate as follows:

$$\hat{\tau}(k+1) = \hat{\tau}(k) + \gamma e(k) \qquad (12)$$

where e(k) is the timing error signal at the kth instant and γ is related to the noise equivalent bandwidth B_L as follows[1]
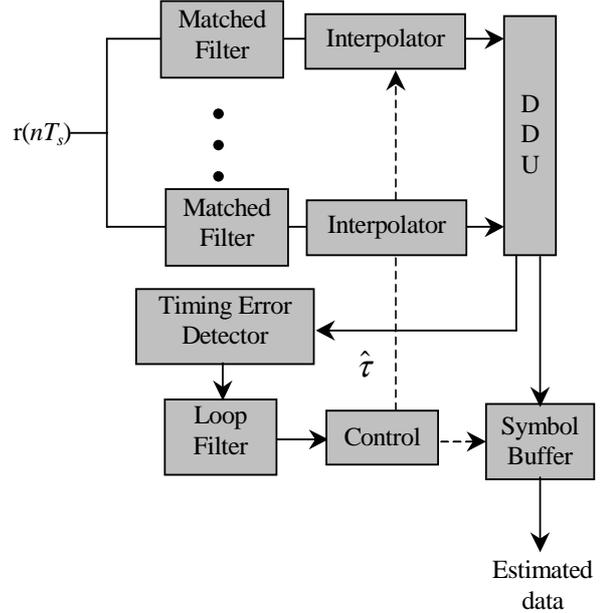

Figure 1 The structure of MTMDS

$$B_L T = \frac{\gamma A}{2(2-\gamma A)} \qquad (13)$$

where A is the slope of S-curve when the timing error is equal to zero. The estimated timing epoch is produced at the symbol rate. The integer part of the estimated timing epoch is used to select one of the symbol decisions from symbol buffer as the estimated symbols are obtained at symbol rate; the fractional part is used for fine timing adjustment. The difference between the novel synchroniser and the conventional one is that the latter decimates the matched filter output to 1 or 2 samples per symbol and it does not have a DDU.

III. HANGUP DETECTION AND CORRECTION

Figure 2 shows the S-curve for different numbers of samples per symbol. From Figure 2, we notice that different numbers of samples per symbol will have different hangup regions. A vertical line drawn from the critical points in Figure 2 identifies the hangup

region and non-hangup region. The critical point is found to be at

$$\left|\frac{\delta}{T}\right| = \frac{1}{2N}(N-K) \qquad (14)$$

where δ is the timing error, T is the symbol period, N is the number of samples per symbol and K is the distance (in terms of number of samples) on the x-axis (i.e. time axis) between the 2 points where the differential is calculated. Thus, we know the hangup region is at
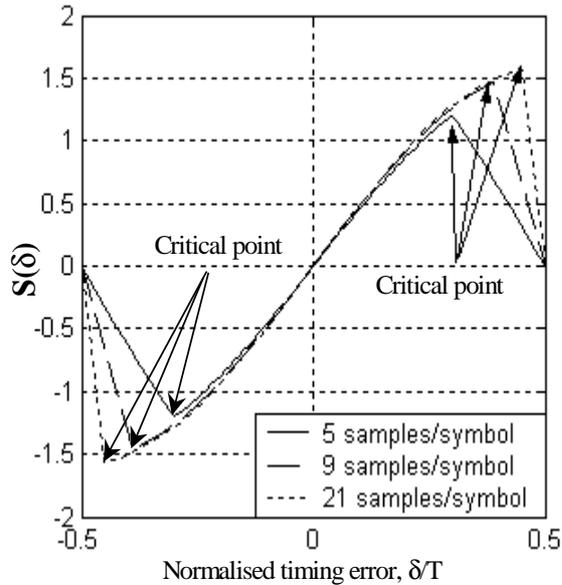

Figure 2 S-curve for different numbers of samples/symbol.

$$\left|\frac{\delta}{T}\right| > \frac{1}{2N}(N-K) \qquad (15)$$

In order to detect a hangup region, we need to find the difference between the current sampling point and the position of the peak. This is illustrated in Figure 3. Note that this could be done only if all the N samples were preserved after the matched filter. This requires a combination of peak search MDS [5]-[6] and MTMDS, now we called hybrid MDS (HMDS). The structure of HMDS is shown in Figure 4. The peak search unit simply searches for the position of the peak, and then the timing error detector will calculate the distance between it current sampling point and the peak position. If (15) is satisfied, then a hangup is declared and the current sampling point is immediately changed to the position of the peak. If hangup is not declared, then the operation is similar to MTMDS.

IV. SELF-NOISE REDUCTION

Self-noise is caused by the inter-symbol interference (ISI) between the raised-cosine pulses. The self-noise in the symbol synchroniser increases when the rolloff

of the raised cosine pulse decreases. For a rolloff of 1.0, the main contribution of self-noise is due to the previous symbol and the next symbol. Thus, by assuming that the pulse duration greater than $2T$ is negligible, there are 3 possible cases:

i)   If all three symbols have the same polarity, then no timing information is available.
ii) If only one of the symbol (i.e. either the previous or the next symbol) has similar polarity to the current symbol then wrong timing information is obtained.
iii) If both the previous and the next symbols have the opposite polarity to the current symbol, then the timing information is accurate, provided that the timing error is small.

The option (iii) is what we strive to achieve. In MFSK, the data is conveyed via selecting the frequency tone. For each MFSK symbol, we invert the phase of the frequency tone so that the phase of successive MFSK symbols alternates between 0 and π. We term this phase-modulated-M-ary-frequency-shift-keying (PM-MFSK). Since the phase modulation is independent of the data, option (iii) is satisfied for all possible data sequences. Since this synchroniser reduces self-noise, we term this self-noise cancellation MDS (SCMDS). Minor modification has to be made to the symbol synchroniser when PM-MFSK is applied. The modification made is shown in Figure 5. The phase-modulated output of the matched filter can be removed by using a nonlinearity, such as a squarer or an absolute function, but these methods introduce more thermal noise into the system. Thus, an alternate phase demodulator (APD) is used instead to remove phase modulation.
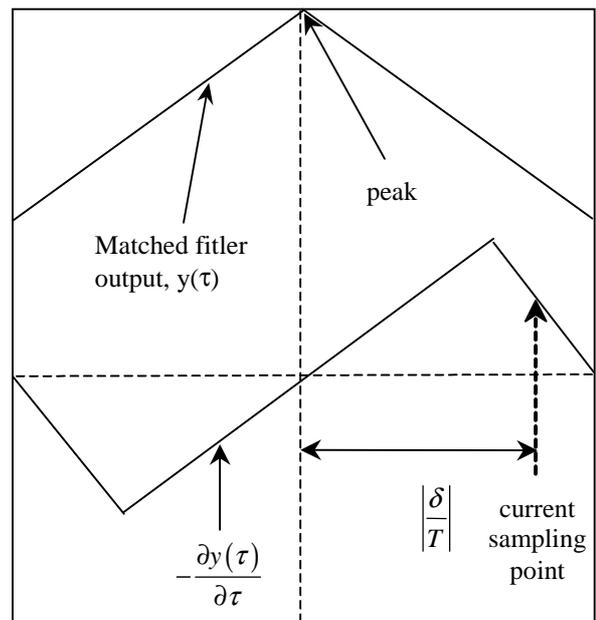

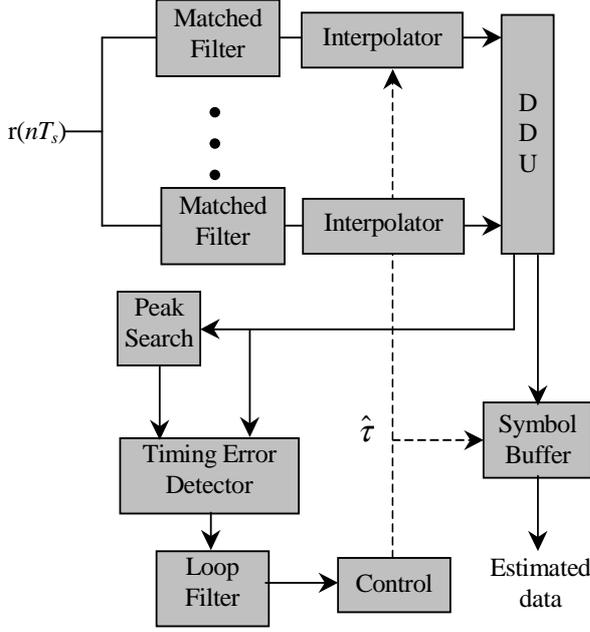**Figure 3** The relationship between the matched filter output and S-curve.
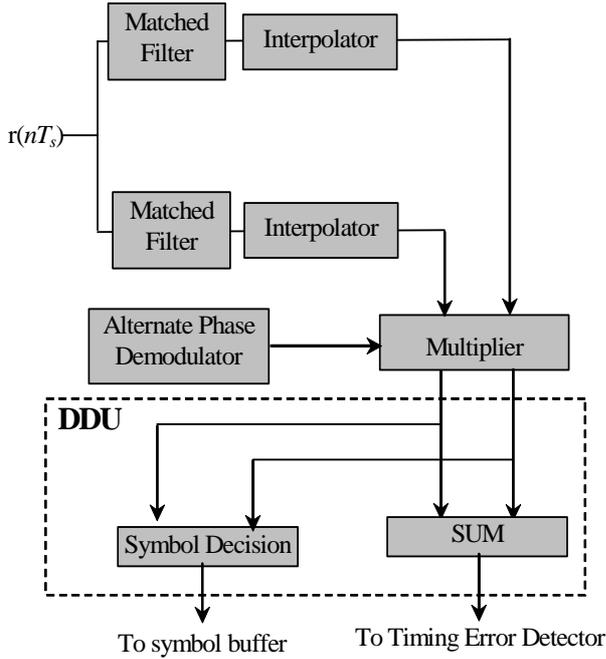
Figure 4 The structure of HMDS.

Figure 5 The structure of SCMDS.

In order to reduce timing error variance in the steady state, the contribution of ISI from the previous symbols must be the same as the next symbols so that the current pulse shape remains symmetrical and the differential at the optimum point of a symmetrical pulse is zero (i.e. the error signal is zero). Therefore, all the matched filter outputs have to be summed since the previous pulses and the future pulses might be located in different matched filter branches. This means that we now have a non-decision-directed (NDD) ML symbol synchroniser. Although this

introduces more thermal noise into the system, it is unavoidable. Consequently, self-noise cancellation MTMDS (SCMTMDS) and self-noise cancellation HMDS (SCHMDS) were developed by applying SCMDS to MTMDS and HMDS respectively.

V. PERFORMANCE ANALYSIS

Normalised timing error variance is given as [1]

$$\sigma_t^2 = \frac{1}{T^2} \sum_{m=-\infty}^{\infty} R_n(m)\eta(m) \qquad (16)$$

where $R_n(m) = E\{n(k+\text{m})n(k)\}$ is the autocorrelation function of the noise and $\eta(m)$ is the convolution of $h(k)$ with $h(-k)$, where **h** is the loop filter response to $n(k)$, i.e.

$$\eta(m) = \sum_{i=-\infty}^{\infty} h(i)\,h(i-m) \qquad (17)$$

After some manipulation, it is found that [1]

$$\eta(m) = \frac{\gamma}{A(2-\gamma A)}\ (1-\gamma A)^{|m|} \qquad (18)$$

where A is the slope of the S-curve at a timing error equal to zero.

$$A = -q''(0) \qquad (19)$$

and $q(t) = g(t) \otimes g_{MF}(-t)$ is the convolution of the root-raised cosine pulse with the matched filter response. Then, substituting into (16) yields

$$\sigma_t^2 = \frac{\gamma}{A(2-\gamma A)T^2} \sum_{m=-\infty}^{\infty} R_n(m)\ (1-\gamma A)^{|m|} \quad (20)$$

Substituting (13) into (20) we have

$$\sigma_t^2 = \frac{2B_L T}{A^2 T^2} \sum_{m=-\infty}^{\infty} R_n(m)\ (1-\gamma A)^{|m|} \qquad (21)$$

The computation of the timing error variance σ_t^2 requires a knowledge of the autocorrelation $R_N(m)$ of the noise. Since the self-noise $n_s(k)$ and the thermal noise $n_t(k)$ are uncorrelated, we have

$$R_n(m) = R_t(m) + R_s(m) \qquad (22)$$

Now considering on $R_t(m)$: the noise from different matched filter branches is assumed to be uncorrelated; thus

$$R_n(m) \ = \ \begin{cases} E\{n_t^2(t)\} & m = 0 \\ 0 & m \neq 0 \end{cases} \qquad (23)$$

To evaluate the noise variance, we need the Fourier transform of $g'(-t)$ which is found to be $-j2\pi f\,G^*(f)$, where $G(f)$ is the Fourier transform of $g(t)$. Thus, the noise variance is given by [1]

$$\sigma_n^2 = E\left\{n_t^2(t)\right\} = \frac{N_0}{2} \cdot 4\pi^2 \int_{-\infty}^{\infty} f^2 \mid G(f)\mid^2 \; df \quad (24)$$

$N_0/2$ is the double-sided power spectral density of additive white Gaussian noise. Note that the noise variance for PM-MFSK is M time larger than (24) since the noise from the M matched filters branches is summed

$$\tilde{\sigma}_n^2 = M \cdot E\left\{n_t^2(t)\right\} = \frac{MN_0}{2} \cdot 4\pi^2 \int_{-\infty}^{\infty} f^2 \mid G(f)\mid^2 \; df$$
$$(25)$$

Assuming that the self-noise is negligible, and collecting terms from (21), (23) and (24), the timing error variance is given by

$$\sigma_t^2 = \frac{N_0 B_L}{A^2 T} \cdot 4\pi^2 \int_{-\infty}^{\infty} f^2 \left|G(f)\right|^2 \; df \quad (26)$$

Then, substituting A from (19), we have

$$\sigma_t^2 = \frac{N_0 B_L}{q''^2(0)T} \cdot 4\pi^2 \int_{-\infty}^{\infty} f^2 \left|G(f)\right|^2 \; df \quad (27)$$

and recognising $q(t) = g(t) \otimes g_{MF}(-t)$, it can be seen that $q''(t)$ has the Fourier transform $-4\pi^2 f^2 \left|G(f)\right|^2$ and, hence, $q''(0)$ can be written as

$$q''(0) = -4\pi^2 \int_{-\infty}^{\infty} f^2 \left|G(f)\right|^2 df \quad (28)$$

Also the signal energy is given by [1]

$$E_s = \int_{-\infty}^{\infty} \left|G(f)\right|^2 df \quad (29)$$

substituting (28) and (29) into (27) produces

$$\sigma_t^2 = \frac{B_L T}{4\pi^2 \xi} \cdot \frac{1}{E_s / N_0} \quad (30)$$

where ξ is an adimensional coefficient given by [1]

$$\xi = T^2 \frac{\int_{-\infty}^{\infty} f^2 \left|G(f)\right|^2 df}{\int_{-\infty}^{\infty} \left|G(f)\right|^2 df} \quad (31)$$

It is also given that [1]

$$B_L T = \frac{1}{2L_0} \quad (32)$$

Hence, by substituting (32) into (30), we have

$$\sigma_t^2 = \frac{1}{8\pi^2 \xi L_0} \cdot \frac{1}{E_s / N_0} \quad (33)$$

which is the well-known modified Cramer-Rao bound (MCRB) [1]. Hence, MTMDS converges to the MCRB when self-noise is negligible. Using the same procedure, but replacing (24) with (25) we have the timing error variance for SCMDS

$$\sigma_t^2 = \frac{M}{8\pi^2 \xi L_0} \cdot \frac{1}{E_s / N_0} \quad (34)$$

which is M time larger than the MCRB.

VI. PERFORMANCE EVALUATION

The performances of the 4 developed symbol synchronisers MTMDS, HMDS, SCMTMDS and SCHMDS were evaluated and compared using performance measures such as acquisition time required and timing error variance. Only 5 samples per symbol were used for an alphabet size of 2 and the channel was AWGN. L_0 was chosen to be 100.
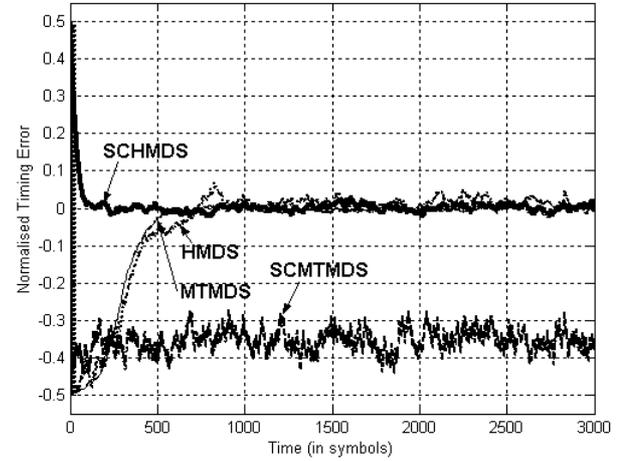
A. Acquisition Time Required

Figure 6 Acquisition time required.

In the simulation, we let the sampling start at the worst possible sampling position which is when the normalised timing error is equal to ±0.5. In other words, sampling at the boundary of the symbols. Random data was used and $E_b/N_0 = 15$ dB. The result is shown in Figure 6. MTMDS acquires synchronisation after approximately 500 symbols; HMDS only acquires synchronisation after approximately 750 symbols; HMDS performs worse

than MTMDS because it is severely affected by self-noise. SCMTMDS requires the longest acquisition time; as we can see from the result, it achieves a normalised timing error of approximately -0.35 after 3000 symbols. This shows that MTMDS has a faster acquisition time when the self-noise is present. SCHMDS has the best performance; it acquires synchronisation after approximately 100 symbols. This shows the proposed anti-hangup algorithm works properly when the self-noise is removed.
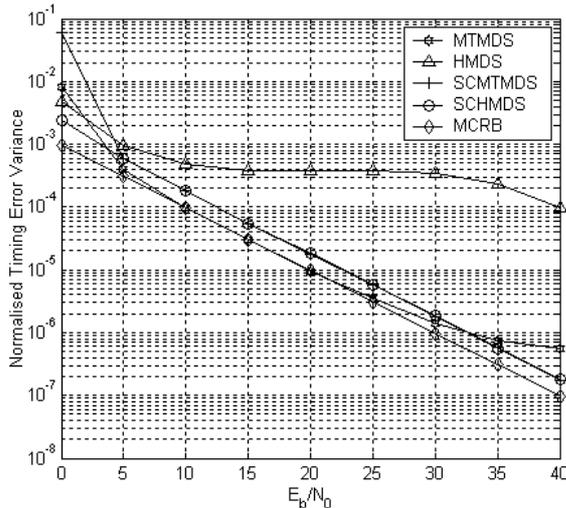
B. Timing Error Variance

Figure 7 Timing error variance.

The timing error variance shown in Figure 7 is normalised by the symbol period:

$$\sigma_t^2 = \frac{(\tau - \hat{\tau})^2}{T^2} \qquad (35)$$

The HMDS has the worst performance because it is severely affected by self-noise due to the repeated symbols. MTMDS converges to the MCRB when the thermal noise dominates, but diverges from the bound at high E_b/N_0 due to self-noise. It is shown that SCHMDS not only has a fast acquisition property, but it has a better timing error variance over SCMTMDS at low E_b/N_0. This is because the timing error estimate is determined by the joint peak search algorithm and timing error detector which makes SCHMDS more robust to noise. SCMTMDS has the worst performance at 0 dB because it is most susceptible to noise. It is worse than MTMDS because its thermal noise variance is larger than the thermal noise variance in MTMDS by a factor of *M*. Nevertheless, the performance of SCMTMDS is the same as SCHMDS when $E_b/N_0 > 5$ dB. Since we simulated for *M*=2, (34) should be approximately 3 dB worse than MCRB. Indeed, from the result, we can see that the performance of SCHMDS and SCMTMDS are approximately 3 dB worse than MCRB at $E_b/N_0 > 5$ dB. This demonstrates that SCHMDS and SCMTMDS do converge asymptotically to a lower

bound indicated by (34) and it also shows that (34) is valid. Both SCHMDS and SCMTMDS have better performance than MTMDS at $E_b/N_0 > 32.5$ dB which indicates the domination of self-noise over thermal noise at high E_b/N_0.

VII. CONCLUDING REMARKS

An improved version of TMDS is developed. The advantages of MTMDS over TMDS include an ability to implement fine timing adjustment and lower complexity, since only 1 sample per symbol is needed to derive the timing estimates; it works even when T/T_s is irrational. Nevertheless, MTMDS is quite similar to the symbol synchroniser described in [1], except the latter was not developed for MFSK systems and it does not have a DDU. HMDS was developed to remove synchronisation hangup, but the objective was not achieved because it is severely affected by self-noise. Nevertheless, SCHMDS successfully removes synchronisation hangups when the self-noise is removed. Both SCMTMDS and SCHMDS are almost self-noise free but they are susceptible to thermal noise because the summation of all matched filter outputs increases the thermal noise variance by a factor *M*, where *M* is the alphabet size. There is no symbol synchroniser that is superior under all conditions. The best compromise is to first use SCHMDS to acquire symbol synchronisation since it has the fastest acquisition time. After symbol synchronisation is acquired, we switch either to MTMDS or SCHMDS depending on channel conditions.

VIII. REFERENCES

[1] U. Mengali, A. N. D'Andrea, *Synchronization Techniques for Digital Receivers*, Plenum Press, 1997.

[2] H. Meyr, M. Moeneclaey, S. A. Fechtel, *Digital Communication Receivers: Synchronization, Channel Estimation, and Signal Processing*, John Wiley & Sons, Inc., 1998.

[3] M. Oerder, "Derivation of Gardner's timing-error detector from the maximum likelihood principle," *IEEE Trans. on Commun.,* Vol 35,pp.684-685 1987.

[4] F.M. Gardner, "A BPSK/QPSK Timing-Error Detector for Sampled Receivers," *IEEE Trans. Commun.*, vol. COM-34, no. 5, pp. 423-429, 1986.

[5] S. M. Brunt, *Comparison of Modulation Derived Synchronisation and Conventional Symbol Synchronisation Techniques in Time Dispersive Channels*, PhD Thesis, University of Leeds, 1998.

[6] C. D. Lee, S.Brunt, M. Darnell, "Comparison of Various Types of Modulation-Derived Synchronisers under Low Sampling Rate Conditions", *5th International Symposium on Communication Theory and Applications*, Ambleside, July 1999.